

# The simplification of the electron-ion many body problem.

## $N$ -representability of the pair densities obtained via a classical-map for the electrons.

M.W.C. Dharma-wardana

National Research Council of Canada, Ottawa, Canada, K1A 0R6 \*

(Dated: November 11, 2019)

The classical map hypernetted-chain (CHNC) method for interacting electrons uses a kinetic energy functional in the form of a classical-fluid temperature. Here we show that the CHNC generated two-body densities and pair-distribution functions (PDFs) correspond to  $N$ -representable densities. Comparisons of results from CHNC with quantum Monte Carlo (QMC) and Path Integral Monte Carlo (PIMC) are used to validate the CHNC results. Since the PDFs are sufficient to obtain the equation of state or linear-response properties of electron-ion systems, we apply the CHNC method for fully classical calculations of electron-ion systems in the quantum regime, using hydrogen at 4000K and 350 times the solid density as an example since QMC comparisons are available. We also present neutral pseudo-atom (NPA) calculations which use rigorous density-functional theory (DFT) to reduce the many nuclear problem to an effective one-ion problem. The CHNC PDFs and NPA results agree well with the ion-ion, electron-ion and electron-electron PDFs from QMC, PIMC, or DFT coupled to molecular dynamics simulations where available. The PDFs of a 2D electron-hole system at 5K are given as an example of 2D ‘warm dense’ matter where the electrons and the counter particles (holes) are all in the quantum regime. Basic methods like QMC, PIMC or even DFT become prohibitive while CHNC methods, being independent of the number of particles or the temperature, prove to be easily deployable.

PACS numbers: 31.10.+z, 71.10.-w, 71.15.Nc, 72.20.Ht

### INTRODUCTION

The wavefunction  $\Psi(\{\vec{r}_i\}, \{\sigma_i\}, \{\vec{R}_j\})$  of an  $N$ -electron quantum system depends on  $3N$  space coordinates  $\vec{r}_i$ , spin  $\sigma_i$ , and the coordinates  $\{\vec{R}_j\}$  specifying the positions of the nuclei. In the following at first the ions are treated as passively providing an ‘external potential’ to the electrons, so that we only have an electron system placed in the ‘external potential’ of the ion subsystem. Subsequently, the two component system of interacting electrons and nuclei are treated.

In the general case with electrons with a one-body density  $n(\vec{r})$  and nuclei at a density  $\rho(\vec{r})$ , we have three many-body interaction terms in the Hamiltonian, viz.,  $V_{ee}$ ,  $V_{ei}$ , and  $V_{ii}$ . Density functional theory (DFT) can be used to reduce each of these three terms to three effective onebody interactions and three corresponding exchange-correlation functionals. That is, a full DFT reduction of the electron-ion manybody problem will involve the familiar  $e$ - $e$  exchange-correlation functional  $F_{xc}^{ee}$  as well as two additional functionals  $F_{xc}^{ei}$  and  $F_{xc}^{ii}$ . Since ions behave as classical particles under normal conditions,  $F_{xc}^{ii}[\rho(r)]$  is simply a correlation functional  $F_c^{ii}$ , with exchange effects being normally of no importance, even if the ions were fermions or bosons. However, if the positively charged particles are not nuclei, but ‘holes’ in semiconductor energy bands at ambient temperatures, positrons or muons, exchange effects have to be included.

In a complete DFT description of, say, a fluid of electrons and carbon nuclei, the many-body problem would be reduced to a single ‘Kohn-Sham electron’ interacting with a single ‘Kohn-Sham carbon ion’ via Coulomb inter-

actions and three coupled XC-functionals. In effect, the total electron-ion problem can be reduced to an effective ‘hydrogenic’ problem. Such a model is already available, mainly for extended systems like fluids and metallic solids, in the implementation of the neutral pseudo atom (NPA) model that was initially introduced into solid state physics [1] using linearly screened ions. Ions screened by a DFT-generated non-linear electron density were introduced by Dagens [2], and then into plasmas and fluids [3] mainly using cluster expansion models for dilute superposed densities of ions, but without recourse to an ion-ion correlation functional. The NPA was reformulated using more systematic DFT arguments in Ref. [4] where explicit ion-ion and electron-ion correlation functionals were introduced.

A further level of simplification, going beyond the NPA model is to replace the quantum electrons by an equivalent classical representation of electrons [5]. In effect, such models replace the quantum kinetic energy functional by a functional for an ‘effective temperature’ of an ‘equivalent’ classical system. Then the PDFs can be determined using classical molecular dynamics (MD) simulations or classical integral equations rather than those of quantum systems which involve fermion sign problems, problems of evaluation of multi-center integrals and large basis sets. Thus, even at zero temperature, even DFT calculations scale non-linearly with the number of particles, and rapidly become prohibitive at finite temperatures, while classical methods remain feasible.

Most DFT calculations only use the  $e$ - $e$  XC-functional and make no recourse to  $F_{xc}^{ei}$  and  $F_c^{ii}$ . This is perhaps because the construction of an XC-functional even for

electrons has been a major task since the inception of density functional theory. However, the three needed XC-functionals can be formally expressed in terms of the three pair-distribution functions  $g_{aa'}(\vec{r}, \vec{r}')$  where  $a$  stands for particle species  $e$ , or  $i$ . This defines fully non-local functionals most appropriate to the given calculation. In fact, if the three pair distribution functions (PDFs) were known, *all* static quantum properties and thermodynamic properties as well as linear transport properties (e.g., electrical conductivities) can be determined without having to know the manybody wavefunction. Hence it would be a great simplification of the electron-ion manybody problem if there were accurate methods for the direct determination of the PDFs via “orbital-free” methods.

The objective of the paper is to demonstrate a method where (a) it is shown that calculations using a classical map for electrons provide results for the three PDFs having an accuracy quite competitive with those from DFT in ‘difficult’ regimes like warm dense matter; (b) the PDFs obtained using the classical map hypernetted-chain technique satisfy the criteria for  $N$ -representability [6, 7].

$N$  representability stipulates that any directly determined PDF or two-body density must be such that it is the result of integrating out the space and spin coordinates of all but two of the particles from the square of a many-body wavefunction (which is unknown). Of course,  $N$ -representability of a two-body density does not guarantee that it is the one with minimum energy, but only that the PDF or two-body density is a reduction of an  $N$ -body wavefunction.

It can perhaps be argued that current rapid developments in computer technology have made attempts at simplifications of the electron-ion problem less relevant. However, even today, DFT calculations are unable to provide all three PDFs  $g_{a,a'}(\vec{r}, \vec{r}')$  even for uniform systems like fluids or electron-hole layers, even at zero temperature. Quantum Monte Carlo (QMC) and path integral Monte Carlo (PIMC) methods become major calculational projects when applied even to electron-proton systems at finite  $T$ . In this study we present examples of competitively accurate calculations using a classical map approach capable of reproducing such heavy computations ‘on a laptop’ in minutes, without the use of *ad hoc* models and using only the temperature, density and nuclear charge as inputs, for a wide class of problems where these methods apply.

## SURVEY OF THE THEORY

Usually the ions behave ‘classically’, while the electrons are quantum mechanical. We seek to represent the electrons even at the extreme quantum limit of  $T = 0$  by an ‘equivalent’ classical Coulomb fluid (CCF), only in the limited sense of having the same pair distribution

functions (PDFs) as the electron system.

The many-electron wavefunction contains significantly more information than necessary for calculating measurable properties of physical systems. As  $N$  becomes large, the solution of the many-particle Schrödinger or Dirac equation, or their QMC or PIMC implementations become numerically prohibitive. A way out is presented by the Hohenberg-Kohn theorem of density functional theory (DFT), which asserts that the ground-state energy  $E$  of the  $N$ -particle system is a functional of just the *one-body* electron density  $n(\vec{r}, \sigma)$  [9–11].

$$n(\vec{r}, \sigma) = \sum_{i=2}^N \int d\vec{r}_2 \dots d\vec{r}_N |\Psi(\vec{r}_1, \dots, \vec{r}_N, \{\sigma_i\})|^2, \quad (1)$$

From now on we consider a paramagnetic electron fluid and suppress spin indices unless we consider effects explicitly dependent on spin-resolution.

The Hohenberg-Kohn theorem is a counter-intuitive result since the many-particle Hamiltonian

$$H = T + V(\vec{r}) + \sum_{i < j} V_{ee}(\vec{r}_i, \vec{r}_j) \quad (2)$$

explicitly contains the electron-electron Coulomb potential – a two-body interaction. The many-body effects of this interaction, as well as corrections arising from the kinetic energy operator  $T$  acting on the many-body wavefunction  $\Psi$  are contained in a one-body energy functional known as the XC-functional of DFT, viz,  $E_{xc}([n])$ . Kohn and Sham modeled the XC-functional using results for the uniform electron liquid (UEL) that we consider here. The Hartree energy of the UEL is zero, and the exchange energy component  $E_x$  of the Hartree-Fock energy is known explicitly. In fact, it is given at arbitrary temperatures in parametrized form in Ref. [8]. The correlation energy  $E_c$  is usually defined as including all contributions to the total energy  $E_T$  beyond the Hartree-Fock energy  $E_{HF}$ , (c.f., Eq. 6.107 of Ref. [11]).

$$E_c = E_T - E_{HF} \quad (3)$$

The grouping of  $E_x$  and  $E_c$  together is needed (especially for free-electron systems like metals and plasmas at finite- $T$ ) to accommodate important cancellations between the two terms [8]. At finite- $T$  we replace the internal energies  $E$  in Eq. 3 by their Helmholtz free energies  $F$ . Furthermore,  $F_x, F_c$  occur as the sum in direct evaluations of XC-energies from the PDF [12]. Thus  $F_x, F_c$  are grouped together in the XC-functional  $F_{xc}$  whose functional derivative with respect to the one-body density gives the Kohn-Sham one-body XC-potential.

### Kohn-Sham theory, one-body and two-body densities

The Hohenberg-Kohn theory posits that the exact ground state one-body density  $n(\vec{r})$  is precisely the one

which minimizes the ground state energy within a constrained search scheme. Its extension to finite- $T$  [13] states that the Helmholtz free energy  $F$  of the system is a functional of the one-body density, and that  $F$  is a minimum for the true density. The finite- $T$  theory is considered to be more robust than the  $T = 0$  theory, e.g., when magnetic fields are included [14, 15].

It was recognized prior to DFT that the ground state energy can be expressed entirely via the two-body density  $n(\vec{r}_1, \vec{r}_2)$ , but a reduction to a one-body functional was not suspected. The two-body density matrix is obtained by integrating all but two of the space and spin variables of the  $N$ -body density, i.e.,  $|\Psi(\{\vec{r}_i\}, \{\sigma_i\})|^2$ . This is also known as the two-particle reduced density matrix (2-RDM), and identifies with the PDF itself (depending on the prefactors used). The pair-distribution function  $g(\vec{r}_1, \vec{r}_2)$  reduces to  $g(r)$  for a uniform system, and gives the probability of finding a second particle at the radial distance  $r$ , with the first particle at the origin.

The one-body density in a system where the origin of coordinates is attached to one of the particles automatically becomes a 2-body density in the laboratory frame, and hence the PDF of homogeneous systems, e.g., a uniform Coulomb fluid, can be used to display the inherent particle correlations in a uniform fluid.

$$n(\vec{r}_1=0, \vec{r}_2=\vec{r}) = \bar{n} g_{12}(r).$$

While placing the origin on a classical particle is possible, so identifying a specific electron in the quantum problem is not possible.

### The $N$ -representability condition on the two body density matrix.

In 1955 Mayer proposed [16] to compute the ground-state energy of  $N$ -electron systems variationally as a functional of the two-electron RDM, i.e., the PDF, instead of the many-body wavefunction. Both  $\Psi$ , and the 2-RDM are unknown, but, unlike the wavefunction, the 2-RDM has the advantage that its application scales polynomially with the number  $N$  of electrons. However, the 2-electron RDM must be a reduction of an  $N$ -body wavefunction for it to be a physically acceptable 2-density. Otherwise, the ground state energy for  $N > 2$  can even fall below the true ground state energy during a variational calculation. So the 2-electron RDM must be constrained to represent an  $N$ -electron wavefunction. Coleman called these constraints  $N$ -representability conditions [6]. The Hohenberg-Kohn minimization must be constrained to satisfy the requirements of  $N$ -representability [17, 18]. We do not present the mathematical constraints enumerated by mathematicians here as we will not use them. Instead, we propose to directly link our CHNC methods to an underlying  $N$ -representable density.

The  $N$ -electron problem when treated in the grand canonical formalism uses a chemical potential  $\mu$  and an explicit number of electrons is used only in the canonical ensemble. The passage to a canonical ensemble requires an ‘inversion’ of thermodynamic functions from the  $\mu$  representation (see Ref. [8]). Such issues are irrelevant to the  $N$ -representability problem as we can choose to work entirely in the canonical ensemble.

### Kinetic energy functionals

The Hohenberg-Kohn method works directly with the density and does not use a Kohn-Sham equation. The implementation of DFT used in Kohn-Sham theory [10] maps the interacting electrons to a set of non-interacting electrons at the *interacting density*, and calculates the ‘Kohn-Sham’ one-electron wavefunctions  $\phi_j(r)$  using some approximation, e.g., a local-density approximation (LDA) to the exchange-correlation potential based on the uniform electron fluid. Hence the corresponding many-body wavefunction is a single Slater determinant at  $T = 0$ , and the Kohn-Sham theory gives rise to the  $N$ -representable density  $n(r)$  given by:

$$n(r) = \sum_j |\phi_j(r)|^2 f(\epsilon_j). \quad (4)$$

At  $T = 0$  the Fermi occupation factors  $f(\epsilon_j)$  are unity or zero for occupied and unoccupied states. Hence the summation at  $T = 0$  is over occupied states.

At finite  $T$  the many body wavefunction  $\Psi$  can be written as a sum over a set of Slater determinants as done in the method of configuration interactions (CI). Thus, if there are  $n$  electrons we need  $N \gg n$  orthonormal functions, e.g., Kohn Sham functions  $\phi_j$  such that the corresponding Fermi occupation factor of the highest energy state used is deemed to be negligible. This is the statistical average over many configurations, and the actual occupancies of the onebody states in each electronic configuration are unity or zero. We can construct  $N!/\{n!(N-n)!\}$  determinants out of the onebody states. All these determinants contain (or omit) orbitals that have unit (or zero) occupations. However, the squares of the coefficients of these determinants, and the occurrence of the orbitals in the determinants give rise to the fractional Fermi factors contributing to the density in Eq. 4.

Alternatively, the Fermi factors are simply given as the statistical weights of the diagonal elements of the  $N$ -representable 2-RDM constructed from  $\Psi$  in the basis of  $\phi_j$  one-body functions. Hence, the finite temperature case can also be re-stated as a discussion in terms of properties of Slater determinants, as is the case for  $T = 0$ . In practical calculations at finite- $T$  the required basis sets become rapidly prohibitive as  $T$  increases. Thus plane wave basis sets cut off at 500-1000 eV are needed, even

with ultra-soft pseudopotentials, in typical applications of DFT for warm-dense-matter [19]. CI calculations using  $\Psi$  become impossible in such cases.

The classical map simplifies the DFT problem further and works with a classical electron system at a classical fluid temperature  $T_{cf}$ . The latter is constructed to include the physical temperature  $T$  as well as a kinetic-energy quantum correction brought in via a quantum temperature  $T_q$  to be discussed below.

The KS  $\phi_j(r), \epsilon_j$  have the physical meaning of being the eigenstates and eigenenergies of the fictitious non-interacting electron map of the interacting electron system, rather than those of the original interacting electron system. The Kohn-Sham procedure guarantees the  $N$ -representability of the density by treating the kinetic energy operator explicitly, without using a kinetic energy (K.E.) functional as in Hohenberg-Kohn DFT.

The simplest K.E. functional is used in Thomas-Fermi theory. Extensions of Thomas-Fermi theory under the name of ‘orbital-free’ DFT, as well as practical applications continue to be relevant [11, 20–24]. Many formulations use the von Weizsäcker ansatz where just one orbital, viz.,  $\phi(r) = \sqrt{n(r)}$  is used in a Schrödinger-like equation to obtain the kinetic energy. However, the non-local nature of the K.E. operator continues to be a great stumbling block. The excellent review by Carter [20], though littered with many acronyms, shows the highly heuristic nature of the search for a K.E. functional that has continued for some four score years.

Several exact requirements on the K.E. functional (such as positivity) and their violation in various implementations have been noted [35, 36]. However, whether ‘orbital-free’ formulations lead to  $N$ -representable densities, or non-negative electron-electron pair-distribution functions etc., do not seem to have been studied. In any case it is known that calculations using K. E. functionals are far less accurate than KS calculations. Furthermore, energies from such calculations may fall *below* the exact energies, as the approximate K.E. functionals may not satisfy  $N$ -representability constraints. In fact, even some Kohn-Sham calculations that use generalized gradient approximations show such anomalies [37].

### The Neutral Pseudo Atom model

A kinetic energy functional is unnecessary for simple ‘one-center’ calculations which are very rapid, and typical in atomic physics or with the neutral-pseudo-atom (NPA) model, originally proposed for solids [2], and adapted to finite- $T$  metallic fluids and plasmas [4, 25–28]. The NPA has been formulated in a number of different ways [29–32]. Here we follow the model of Ref. [26] which is a simplification of [4] and adapted to multi-component finite- $T$  calculations. In these NPA models of electron-ion systems, the many-ion problem is replaced by a ‘one-ion’

problem together with the corresponding ion-ion correlation functional, while the many-electron problem is replaced by a single-electron KS problem.

However, in simulations done with codes like the VASP [33] or ABINIT [34] the many-ion problem is *not* reduced. Instead, they explicitly use some 100-200 nuclear centers, say  $N_I$ , and even up to  $N = N_e \sim 1000$  electrons in thousands of steps of KS and molecular-dynamics (MD) calculations. Hence such methods are extremely expensive and become prohibitive for many problems in warm-dense matter, materials science and biophysics. However, they provide useful benchmarks in simplified limits. Such  $N_I$ -ion quantum calculations can be greatly simplified as follows.

1. By the use of an explicit electron kinetic energy functional of the one-body electron density  $n(\vec{r})$  if an adequate K.E. functional were available.
2. Using a neutral pseudo-atom approach where the  $N_I$  nuclei are replaced by a one-body ion density  $\rho(\vec{r})$  [4, 25], while the electrons are treated as usual as a functional of  $n(\vec{r})$  from KS theory. Since ions are normally classical particles, an ion is chosen as the origin of coordinates with no loss of generality. Two coupled KS-equations for the two subsystems ( $e$ - $i$ ) arise on functional differentiation of  $F$ .

$$\frac{\delta F([n], [\rho])}{\delta [n]} = \mu_e, \quad \frac{\delta F([n], [\rho])}{\delta [\rho]} = \mu_I. \quad (5)$$

The electron and ion chemical potentials appear on the RHS. The first equation reduces to a one-center Kohn-Sham equation for the electrons in the field of the ion at the origin, while the second equation defines a classical distribution around the origin containing an ion-correlation functional, and reduces to a hypernetted chain (HNC) type integral equation [4, 25]. If there are many types of ions, a coupled set of one-center HNC equations appear [26].

This reduction of the electron-ion problem does not invoke the Born-Oppenheimer (BO) approximation, but BO can be implemented by neglecting  $F_{xc}^{ei}[n, \rho]$ . The solution of such one-center equations is numerically extremely rapid, even at finite  $T$ . Such calculations reproduce the PDFs  $g_{cc}(r)$  of, say, molten carbon (or silicon) containing a complex bonding structure that are only exposed by taking ‘snap shots’ in lengthy and expensive DFT-MD simulations. That is, the *one-center* NPA calculations include sufficiently good ion-ion classical correlation functionals such that they are able, e.g., to reproduce the peak in the  $g_{cc}(r)$  that corresponds to the 1.4-1.5Å C-C covalent bond as well the peaks in the  $g(r)$  due to the hard sphere-like packing effects seen in DFT-MD simulations. This is demonstrated in Refs. [27, 28].

3. The NPA approach can also be further simplified by the use of a K.E. functional; but the NPA calculation is so rapid that little is gained on using approximate K.E. functional with their own errors.

Several models use the the name “Neutral Pseudo Atom”, but there are significant differences. Thus Chihara uses a neutral-pseudo-atom construction where he begins from the HNC equation and identifies a ‘quantum’ Ornstein-Zernike (OZ) equation applicable to electrons as well [32]. Its validity for quantum electrons is debatable. Thus Anta and Louis [30] in their implementation of an NPA using Chihara’s ‘quantal HNC (qHNC)’ scheme cautiously avoid the use an  $e$ - $e$  qHNC equation. The NPA approach proposed by the present author and Perrot [4] simply uses DFT for both electrons and ions, and invokes the HNC diagrams, bridge diagrams and the Ornstein-Zernike equation only to construct an ion-ion correlation functional [4, 26].

A simplification of the effort to construct a kinetic energy functional is to look for a classical description of the electrons. This is possible when the bound states have already been treated using some complementary approach like the NPA, or when there are no bound states because the system is highly compressed or at a temperature where such effects can be neglected. If the system is a fluid or plasma, classical integral equations or classical molecular dynamics can be used to obtain the PDFs of the classical-map electrons that are not plagued by Fermion sign problems.

### The classical map hypernetted-chain scheme.

The study of the electron distribution in a uniform electron liquid (UEL) when a ‘test electron’ is placed at the origin leads to the question of the direct calculation of the physically valid  $g_{ee}(r)$  of the UEL rather than for a ‘test particle’. Here the electron kinetic energy functional must satisfy the required constraints, and also avoid any *selection* of an ‘electron’ held at the origin whereby it is made into a specific ‘test particle’. Such a problem does not arise for classical electrons [5].

We recapitulate the classical map hypernetted-chain (CHNC) scheme for the convenience of the reader. It has been used successfully [5, 38–40, 58] for a number of uniform systems, namely, 3D and 2D UELs, electron-proton plasmas [41], warm-dense matter [42], double quantum wells [43] etc. We present arguments to show that the pair-densities obtained via the classical-map technique are  $N$ -representable.

Consider an  $N$  electron system in a volume  $V$  such that  $N/V = \bar{n}$ , forming a uniform electron liquid in the presence of a neutralizing positive uniform background. The electron eigenfunctions for the self-consistent field problem (Hartree as well as Hartree-Fock models) are

simple plane waves.

$$\phi_j(r) = \phi_{\vec{k}\sigma}(\vec{r}) = (\bar{n}/N)^{1/2} \exp(i\vec{k} \cdot \vec{r})\zeta_\sigma. \quad (6)$$

Here  $j$  is an index carrying any relevant quantum numbers including the spin index  $\sigma$  associated with the spin function  $\zeta$ , with  $\sigma = 1, 2$  or ‘up, down’, specifies the two possible spin states. Some of the vector notation will be suppressed for simplicity, as appropriate for uniform liquids with spherical symmetry in 3D and planar symmetry in 2D. The spin index may also be suppressed where convenient.

### The non-interacting pair-distribution function $g^0(r)$

The many-electron wavefunction for non-interacting electrons in a uniform system, as well as for Hartree-Fock (mean-field) electrons is a normalized antisymmetric product of planewaves [44], i.e, a Slater determinant  $D(\phi_1, \dots, \phi_j)$  of  $N$ -plane waves. Its square is the  $N$ -particle density matrix, while the PDF is the two particle density matrix [45]. In the following we assume Hartree atomic units with  $|e| = \hbar = m_e = 1$ , where standard symbols are used.

$$g_{\sigma_1, \sigma_2}(\vec{r}_1, \vec{r}_2) = V^2 \Sigma_{\sigma_3, \dots, \sigma_N} \int d\vec{r}_3 \dots \vec{r}_N D(\phi_1, \dots, \phi_j). \quad (7)$$

If the spins are anti-parallel, then the non-interacting PDF,  $g_{u,d}^0(r)$  is unity for all  $\vec{r}$ . Denoting  $(\vec{r}_1 - \vec{r}_2)$  by  $\vec{r}$ , and  $(\vec{k}_1 - \vec{k}_2)$  by  $\vec{k}$ , we have, for parallel spins,

$$g_{\sigma, \sigma}^0(\vec{r}) = \frac{2}{N^2} \Sigma_{\vec{k}_1, \vec{k}_2} f(k_1) f(k_2) \left[ 1 - \exp(i\vec{k} \cdot \vec{r}) \right] \quad (8)$$

$$f(k) = \left[ 1 + \exp\{(k^2/2 - \mu^0)/T\} \right]^{-1}. \quad (9)$$

Here we have generalized the result to finite  $T$ , where the temperature is measured in energy units. Thus the non-interacting PDFs, i.e.,  $g^0(r)$  are explicitly available at  $T = 0$ , and numerically at finite  $T$ .

$$g_{\sigma, \sigma}^0(r) = 1 - F^2(r) \quad (10)$$

$$F(r) = (6\pi^2/k_F^3) \int f(k) \frac{\sin(kr)}{r} \frac{kdk}{2\pi^2} \quad (11)$$

$$3\text{D, zero } T, = 3 \frac{\sin(x) - x \cos(x)}{x^3}, \quad x = k_F r. \quad (12)$$

The equations contain the Fermi momentum  $k_F$  which is defined in terms of the mean density  $\bar{n}$  and the corresponding electron Wigner-Seitz radius  $r_s$ . Here we have assumed equal amounts of up and down spins (paramagnetic case) and defined the Fermi wavevector  $k_F$ .

$$k_F = 1/(\alpha r_s), \quad r_s = [3/(4\pi\bar{n})]^{1/3}, \quad \alpha = (4/9\pi)^{1/3}. \quad (13)$$

Similar expressions can be developed for the 2D electron layer [38], two coupled 2D-layers [43] or a two-valley 2D

layer [46] relevant to silicon-metal oxide field effect transistors. The method has also been used successfully to obtain the local-field factors of 2D layers at zero and finite- $T$  [47], and for the study of thick 2D layers which are of technological interest [48].

### THE $N$ -REPRESENTABILITY OF PAIR DENSITIES FROM THE CLASSICAL MAP

We first discuss the non-interacting pair-density and then use its manifest  $N$ -representability to establish the  $N$ -representability of the interacting map.

#### Non-interacting electron gas.

The PDFs  $g_{\sigma,\sigma'}^0(r) = 1 - \delta_{\sigma,\sigma'}F(r)$  calculated in the previous section were derived from the Slater determinant  $D(\phi_1 \dots, \phi_N)$  and hence manifestly  $N$ -representable. At this stage, irrespective of where it came from, we regard  $g^0(r)$  as a classical pair-distribution function for classical electrons interacting by a classical pair potential  $\beta\mathcal{P}(r)$  where  $\beta$  is the inverse temperature. This is the first step in our classical map, and we may now identify one of the classical particles as being at the origin, without loss of generality, in a classical picture of the PDF. Clearly, for anti-parallel spins, i.e.,  $\sigma \neq \sigma'$ , the pair-potential  $\beta\mathcal{P}(r)$  is zero, while it is finite and creates the well-known ‘exclusion hole’ in the PDF of two parallel-spin particles. Hence  $\mathcal{P}(r)$  has been called the ‘Pauli exclusion potential’ and should not be confused with the Pauli kinetic potential that appears in the theory of the kinetic energy functional.

F. Lado was the first to present an extraction of  $\beta\mathcal{P}(r)$  for 3D electrons at  $T = 0$  using the hypernetted-chain (HNC) equation and the Ornstein-Zernike (OZ) equation [49]. Only the dimensionless potential,  $\beta\mathcal{P}(r)$  is determined from the equations. Although the physical temperature  $T$  of the quantum fluid is zero, the temperature of the classical fluid invoked by the map is left undetermined (but nonzero) in the ‘non-interacting’ system. The Pauli exclusion potential for 2D electrons at arbitrary  $T$  was derived in Ref. [38]. Although the quantum electrons are not interacting via a Coulomb potential,  $\beta\mathcal{P}(r)$  becomes a classical manifestation of entanglement interactions which scale as  $r/r_s$ , and hence extend to arbitrarily large distances [50]. Assuming that  $g^0(r)$  can be written as an HNC equation, we have:

$$g^0(r) = \exp[-\beta\mathcal{P}r + h^0(r) - c^0(r)] \quad (14)$$

$$h^0(r) = c^0(r) + \bar{n} \int d\vec{r}' h^0(|\vec{r} - \vec{r}'|) c^0(\vec{r}') \quad (15)$$

$$h^0(r) = g^0(r) - 1. \quad (16)$$

The first of these is the HNC equation, while the second equation is the Ornstein-Zernike relation. These contain

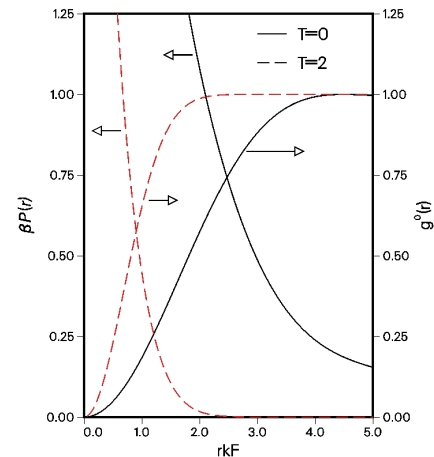


FIG. 1. The exclusion potential, Eq. 17, and the noninteracting PDF,  $g_{\sigma,\sigma}^0(r)$  at  $t = T/E_F = 0$  (solid line) and at  $t = 2$  (dashed line). They are universal functions of  $r/r_s$ . The PDF  $g_{\sigma \neq \sigma'}^0(r) = 1$  as there is no exclusion effect for  $\sigma \neq \sigma'$ .

the direct correlation function  $c^0(r)$  and the total correlation function  $h^0(r)$ . It should be noted that we have ignored the two-component character of the electron fluid (two spin types) in the equations for simplicity, but the full expressions are given in, say, Ref. [5]. These equations can be solved by taking their Fourier transforms, and the Pauli exclusion potential can be obtained by the inversion of the HNC equation. The ‘Pauli exclusion potential’ (PEP)  $\beta\mathcal{P}(r)$  is given by

$$\beta\mathcal{P}(r) = -\log[g^0(r)] + h^0(r) - c^0(r). \quad (17)$$

The PEP is a universal function of  $rk_F$  or  $r/r_s$ . It is long ranged and mimics the exclusion effects of Fermi statistics. At finite  $T$  its range is about a thermal de Broglie wavelength and is increasingly hard-sphere-like as  $r \rightarrow 0$ . The Fourier transform  $\beta\mathcal{P}(q)$  in 3D behaves as  $\sim 1/q$  for small  $q$ , and as  $\sim c_1/q^2 + c_2/q^4$  for large  $q$ .

Plots of  $\beta\mathcal{P}(r)$  and  $g^0(r)$  for a 3D UEL are given in Fig. 1.

We note that the HNC or MHNC integral equation, together with the OZ equation may be regarded as a transformation where, given the dimensionless pair potential  $\beta\phi_{ij}(r)$ , the corresponding PDF, i.e.,  $g_{ij}(r)$  is generated. Similarly, given the  $g_{ij}(r)$ , HNC inversion is the process which extracts the corresponding  $\beta\phi_{ij}(r)$ . The value of  $g(r)$  for the full range of  $r$ , or additional constraints are needed to obtain an unequivocal HNC inversion to extract a valid pair potential from a PDF [51, 52].

## THE INTERACTING SYSTEM AND ITS CLASSICAL MAP

In the previous section we reviewed a classical fluid whose  $g^0(r)$  exactly recovers the PDFs of the non-interacting quantum UEL at any density, spin polarization or temperature. From now on, for simplicity we consider a paramagnetic electron liquid (equal amounts of up spins and down spins) although spin-dependent quantities will be indicated where needed for clarity. Although the quantum liquid was ‘noninteracting’, the classical map already contains the pair potential  $\beta U_{ij} = \beta \mathcal{P}(r)$ .

On addition of a Coulomb interaction  $\beta V_{ij}(r)$  the total pair potential becomes

$$\beta U_{ij}(r) = \beta \mathcal{P}(r) + \beta V_{cou}(r). \quad (18)$$

The temperature  $T = 1/\beta$  occurring in Eq. 18 is as yet unspecified. In quantum systems the Coulomb interaction is given by the *operator*  $1/|\vec{r}_1 - \vec{r}_2|$  which acts on the eigenstates of the interacting pair. It can be shown (e.g., by solving the relevant quantum scattering equation) that the classical Coulomb interaction,  $V_{cou}(r), r = |\vec{r}_1 - \vec{r}_2|$  acquires a diffraction correction for close approach. Depending on the temperature  $T$ , an electron is localized to within a thermal de Broglie wavelength. Thus, following earlier work on diffraction corrected potentials, (e.g., in Compton scattering in high-energy physics), or in plasma physics as in, e.g., Minoo *et al.* [53], we use a ‘‘diffraction corrected’’ potential.

$$V_{cou}(r) = (1/r)[1 - e^{-r/\lambda_{th}}]; \lambda_{th} = (2\pi\bar{m}T_{cf})^{-1/2}. \quad (19)$$

Here  $\bar{m}$  is the reduced mass of the interacting electron pair, i.e.,  $m^*(r_s)/2$  a.u., where  $m^*(r_s)$  is the electron effective mass. It is weakly  $r_s$  dependent, e.g.,  $\sim 0.96$  for  $r_s = 1$ . In this work we take  $m^*=1$ . The ‘‘diffraction correction’’ ensures the correct quantum behaviour of the interacting  $g_{12}(r \rightarrow 0)$  for all  $r_s$ . The essential features of the classical map are

1. The use of the exact non-interacting quantum PDFs  $g_{\sigma,\sigma'}^0(r)$  as inputs.
2. A diffraction corrected Coulomb interaction.
3. The specification of the temperature of the classical Coulomb fluid  $T_{cf}(r_s) = 1/\beta$  as the one that recovers the quantum correlation energy  $E_c(r_s)$ .

The selection of  $T_{cf}$  is a crucial step. This is guided by the Hohenberg-Kohn-Mermin property that the exact minimum free energy is determined by the true one-body electron density  $n(r)$ . Since we are dealing with a uniform system, the Hartree energy  $E_H$  is zero. The exchange energy  $E_x$  is already correctly accounted for by the construction of the classical-map  $g^0(r)$  to be identical with the quantum  $g^0(r)$  at any  $T$  or spin polarization. Hence

the only energy to account for is  $E_c$ . So we choose to select the temperature  $T_{cf}$  of the classical Coulomb fluid to recover the known DFT correlation energy  $E_c$  at each  $r_s$  at  $T = 0$ . Since this is most accurately known for the spin-polarized electron liquid,  $T_{cf}$  is best determined from  $E_c(r_s)$  for full spin polarization. A trial temperature is selected and the interacting  $g(r, \lambda)$  is determined for various values of the coupling constant  $\lambda$  in the interaction  $\lambda V_c(r)$  to calculate a trial  $E_c$  at the given  $r_s$  from the coupling constant integration. The temperature is adjusted until the  $E_c(r_s, T_{cf})$  obtained from the classical fluid  $g(r)$  agrees with the known quantum  $E_c(r_s, T = 0)$ . Given an electron fluid at  $T = 0$ , the temperature of the classical fluid with the same  $E_c$  is called its *quantum temperature*  $T_q$ . This was parametrized as:

$$T_q/E_F = 1.0/(a + b\sqrt{r_s} + cr_s) \quad (20)$$

For the range  $r_s = 1$  to 10,  $T_q/E_F$  goes from 0.768 to 1.198. The values of the parameters  $a, b, c$  are given in Ref. [5].

There is no *a priori* reason that the  $n(r)$ , i.e.,  $\bar{n}g(r)$  obtained by this procedure would agree with the quantum  $\bar{n}g(r)$ , except for the Hohenberg-Kohn theorem that requires  $n(r)$  to be the true density distribution when the energy inclusive of the XC-energy is correctly recovered. Many well-known and often very useful quantum procedures (e.g., that of Singwi *et al.* [54, 55]) for the PDFs lead to negative  $g(r)$  as  $r_s$  is increased beyond unity even into the ‘liquid metal’  $r_s$  range.

However, as shown in Refs. [5, 38, 56] etc., the classical map HNC  $g(r)$  is an accurate approximation to the QMC PDFs then available only at  $T = 0$ . Correlations are stronger in reduced dimensions. The classical map for the 2D UEL was constructed using the modified-HNC (MHNC) equation where a hard-sphere bridge function was used, with the hard-sphere radius determined by the Gibbs-Bogoliubov criterion, as given by Lado, Foils and Ashcroft (LFA) [57]. Other workers [39, 40, 58] have examined different parametrizations than our Eq. 20. Datta and Dufty [59] examined the classical map approach and the method of quantum statistical potentials [60, 61] within a grand-canonical formalism. They proposed using additional conditions (besides the requirement that  $E_c$  is reproduced by  $T_{cf}$ ) to constrain the classical map for warm dense electrons, a topic recently reviewed by Dornheim *et al.* [62].

Although  $E_c$  values at  $T = 0$  were available when the classical map for the UEL was constructed, no reliable XC-functional (beyond RPA) was available for the finite- $T$  electron liquid. Hence we proposed the use of the ‘ $T$  ansatz’:

$$T_{cf} = (T_q^2 + T^2)^{1/2} \quad (21)$$

as a suitable map for the finite- $T$  UEL. This was based on the behaviour of the heat capacity and other thermodynamic properties of the UEL. Furthermore, using

Eq. 21 it became possible to predict the XC-free energy  $F_{xc}(r_s, T)$  as well as the finite- $T$  PDFs of the UEL at arbitrary temperatures and spin polarizations. These were found to agree closely with the  $F_{xc}(r_s, T)$  and PDFs resulting from the Restricted Path Integral Monte Carlo (RPIMC) simulations reported 13 years later by Brown *et al.* [63]. The Brown *et al.* data have been used by Liu and Wu [58] to construct a direct fit of a  $T_{cf}$  that avoids the model used in Eq. 21, by using temperature dependent parameters  $a, b$  and  $c$  in Eq. 20. The RPIMC data have been parametrized by Karasiev *et al.*, Ref. [64]. However, Groth, Dornheim *et al.* [65] presented a new *ab initio* parametrization of  $F_{xc}(r_s, T)$  using accurate data from recently developed finite- $T$  fermionic PIMC methods that deal with the sign problem more carefully and also compensate more systematically for finite-size effects [62]. These agree even more closely with the CHNC data.

Calculations of  $F_{xc}$  using the finite  $T$  parametrization given by Perrot and Dharma-wardana [56] are compared with the Karasiev *et al.* parametrized results, and those of Groth *et al.* in Fig. 2. The classical temperature ansatz of Eq. 21 recovers the highly accurate Groth *et al.* results to within 94 %, i.e., with an error of at most 6%. The parametrizations given by PDW [56], Iyatomi and Ichimaru, and subsequent parametrizations incorporate the high- $T$  Debye-Hückel limit of  $F_c$ , the high- $T$  behavior of  $F_x(T)$ , as well as the behaviour at the  $T = 0$  limit. The PDW fit to the CHNC data fall below the Groth *et al.* data near  $T = 0$  partly because older  $T = 0$  data were used in the CHNC parametrizations. The CHNC method has also been used to construct  $F_{xc}(T)$  for 2D electron layers and used to calculate finite- $T$  local-field factors, PDFs, and related quantities relevant to double quantum wells, metal-oxide field effect transistors and nanostructures; but no finite- $T$  QMC or PIMC benchmarks are currently available for the 2D electron system.

#### **$N$ -representability of the interacting $g(r)$ of the classical map.**

The conditions  $n(r) = \bar{n}g(r) > 0$ , and  $\int n(\vec{r})d\vec{r} = N$  are always satisfied by the classical map. Furthermore, the classical map becomes more accurate as  $t = T/E_F$  is increased, or when  $r_s$  is increased, since quantum electrons become increasingly classical in those limits.

We present two types of arguments to conclude that the  $g(r)$  of the interacting UEL obtained by the classical map is  $N$ -representable. One of them is a formal argument based on CHNC being a “well behaved” transformation of the already  $N$ -representable non-interacting density. The second is a practical demonstration of the implementability of CHNC method and the close agreement with results from QMC, PIMC and other more mi-

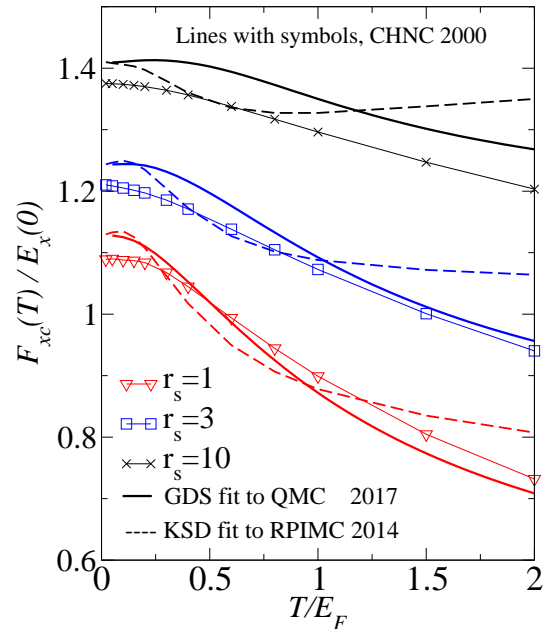


FIG. 2. (Color online) Finite- $T$  exchange and correlation free energy  $f_{xc}(r_s, T)$  scaled by the exchange energy  $E_X = E_x$  at  $T=0$  as a function of the reduced temperature  $t = T/E_F$  in units of the Fermi energy is displayed. The lines with symbols are results from CHNC calculations [56]. The restricted path integral Monte Carlo (RPIMC) data of Brown *et al.*, Ref. [63], as parametrized by Karasiev *et al.* [64] are shown as dashed lines. The thick continuous lines are from the Groth *et al.* parametrization of very accurate fermionic-PIMC data. The temperature range  $t < 1$  is relevant to WDM studies.

croscopic benchmark calculations. Finally, we give an example of a CHNC calculation for electron-hole layers at finite temperatures, as an example of topical technological interest for which QMC, PIMC, and even DFT seem to be quite prohibitive at present.

#### **(1)Argument based on the HNC equation being an $N$ -representability conserving transformation.**

Once the  $g^0(r)$  of the quantum fluid is evaluated we consider a classical fluid which has the same  $g^0(r)$ . The non-interacting  $g^0(r)$  and the corresponding  $n^0(r) = \bar{n}g^0(r)$  of the classical fluid are generated from the homogeneous density  $\bar{n}$  by a transformation where the origin of coordinates is moved to one of the particles. The corresponding transformation of the density profile is written as:

$$n^0(r) = \mathcal{T}_0(r)\bar{n} \quad (22)$$

$$\mathcal{T}_0(r) = \exp[\beta\mathcal{P}(r) + h^0(r) + c^0(r)]. \quad (23)$$

$$(24)$$

The so generated  $n^0(r)$  is  $N$ -representable by its construction from a Slater determinant. Then, in a next step the interacting  $g(r)$  is generated from the  $N$ -representable non-interacting  $g^0(r)$  by a transformation

which can be written as:

$$g(r) = \mathcal{T}_1(r)g^0(r) \quad (25)$$

$$\begin{aligned} \mathcal{T}_1(r) &= e^{[\beta V_{cou}(r) + \{h(r) - h^0(r)\} + \{c(r) - c^0(r)\}]} \\ &= \exp[\beta\{V_{cou}(r) + V_{MF}(r) + V_{xc}(r)\}]. \end{aligned} \quad (26)$$

In effect, the uniform density  $\bar{n}$  has been transformed (by a selection of the origin of coordinates, and by switching on the Coulomb interaction) by a single composite transformation  $\mathcal{T} = \mathcal{T}_1\mathcal{T}_0$  with its components acting one after the other.

In equation 26 we use  $V_{xc}(r)$  to indicate the exchange-correlation correction to the mean-field potential  $V_{MF}(r)$  as discussed in Ref. [4] where explicit expressions for these classical XC-potentials in the HNC approximation are given. These potentials are expected to be well-behaved functions. The diffraction-corrected classical Coulomb potential  $V_{cou}(r)$  has a finite-value at  $r = 0$ , and not singular, unlike the point-Coulomb potential  $1/r$  which is not used in CHNC. Hence we may regard the above transformation as being mathematically equivalent to a type of smooth, or ‘well-behaved’ coordinate transformation of  $\vec{r}$  to another variable  $\vec{s}$ .

$$d\vec{s} = \mathcal{T}(r)\bar{n}d\vec{r} = n(r)d\vec{r}. \quad (27)$$

That is, the initial planewave states  $(\bar{n}/N)^{1/2} \exp(i\vec{k} \cdot \vec{r})$  are transformed to a new set  $(n(\vec{r})/N)^{1/2} \exp(i\vec{q} \cdot \vec{s}(r))$ . It is easily shown that they form a mutually orthogonal complete set. For instance, consider the initial planewave state used in the Slater determinant, i.e.,  $\phi_j(\vec{r}) = \phi_k(\vec{r})$  and consider its transformed state  $\tilde{\phi}_k(\vec{r})$  given below:

$$\phi_k(\vec{r}) = (\bar{n}/N)^{1/2} \exp(i\vec{k} \cdot \vec{r}) \quad (28)$$

$$\tilde{\phi}_k(\vec{r}) = (n(\vec{r})/N)^{1/2} \exp(i\vec{k} \cdot \vec{s}(\vec{r})). \quad (29)$$

We regard  $\vec{k}$  as an arbitrary  $k$ -vector and hence it is sufficient to transform  $\vec{r}$ , while the theory can also be constructed entirely in  $k$ -space in an analogous manner. The transformed wavefunctions  $\tilde{\phi}_k(\vec{r})$  have the following properties:

$$\int \tilde{\phi}_{k'}^*(\vec{r})\tilde{\phi}_k(\vec{r})d\vec{r} = \int \frac{n(\vec{r})}{N} e^{i(\vec{k}' - \vec{k}) \cdot \vec{r}} d\vec{r} \quad (30)$$

$$= \frac{1}{N} \int \exp\{i(\vec{k}' - \vec{k}) \cdot \vec{s}\} \frac{d\vec{s}}{N} \quad (31)$$

$$= \frac{(2\pi)^3}{N} \delta^3(\vec{k}' - \vec{k}). \quad (32)$$

Furthermore,

$$\int \tilde{\phi}_k^*(\vec{r})\tilde{\phi}_k(\vec{r}') \frac{d\vec{k}}{(2\pi)^3} = \frac{\delta^3(\vec{r} - \vec{r}')}{N}. \quad (33)$$

Hence the transformed functions  $\tilde{\phi}_k(\vec{r})$  form a complete orthogonal set. This implies that the initial Slater determinant  $D(\phi_{k_1}, \dots, \phi_{k_N})$  of the noninteracting electron

system transforms to the determinant  $D(\tilde{\phi}_{k_1}, \dots, \tilde{\phi}_{k_N})$  of the interacting system, explicitly showing the  $N$ -representability of the  $n(r) = \bar{n}g(r)$  obtained via the classical map which consists of the application of the two transformations  $\mathcal{T}_1\mathcal{T}_0$ . Furthermore, the transformations commute, in the sense that one may first apply *only* the diffraction corrected Coulomb potential to non-interacting fermions to generate a  $g^c(r)$  for a Coulomb fluid, and then apply the Pauli exclusion potential to generate the fully interacting classical map inclusive of exchange-correlation effects, or *vice versa*. This is equivalent to iterating the HNC equations from the non-interacting state via two different paths, and indeed the two different procedures,  $\mathcal{T}_1\mathcal{T}_0$  and  $\mathcal{T}_0\mathcal{T}_1$  lead to the same final  $g(r)$ .

In the above demonstration we have appealed to the concept of ‘well behavedness’ of the potentials. These have been defined by Lieb to be based on a Hilbert space of potentials  $\mathcal{V} = L^3/2 + L^\infty$  [68]. These are potentials that do not become singular or include infinite barriers, discontinuities etc. The potentials used in CHNC satisfy such concepts of ‘well behavedness’.

What if a phase transition, e.g., a Wigner crystallization, intervenes in passing from the non-interacting to the interacting system? The CHNC procedure for a uniform system will smoothly proceed to the best interacting fluid state (an upper bound to the ground-state energy) and not the lower-energy Wigner crystal state. This is still consistent with the variational principle and  $N$ -representability.

The above analysis confirms the  $N$ -representability of the pair-densities of the interacting uniform electron liquid generated by the classical map presented here. A similar analysis can be given if MD were used to generate the interacting  $g(r)$  via CHNC potentials, instead of using the HNC equation.

## (2)Argument based on the $N$ -representability of the QMC density.

The diffusion quantum Monte Carlo (DQMC) calculations use a Slater determinant together with Jastrow factors, and hence the DQMC procedure is based on an explicit many-body wavefunction whose variation produces a minimum energy and a corresponding  $E_c(r_s)$ . Hence its two-particle reduced density matrix, i.e., the electron-electron PDF is  $N$ -representable; the correlation energy  $E_c$  associated with the  $N$ -representable two-body density is the correlation contribution to the best approximation to the energy minimum as per Hohenberg-Kohn theorem, since the minimum is achieved only for the true density. The CHNC electron-electron PDFs agrees with the DQMC- $g(r)$  with *no attempt at fitting* the PDFs. The only input is the single number  $E_c(r_s)$  at each density introduced via the classical temperature  $T_{cf}$  - a classical kinetic energy. The CHNC electron density  $\bar{n}g(r)$  agrees closely at every  $r$  with those of the  $N$ -representable density  $\bar{n}g_{\text{qmc}}(r)$ . Further more, the CHNC

energies  $E_{xc}(r_s, \zeta)$  at arbitrary spin polarizations  $\zeta$  that were not include in any fits agree with microscopic calculations. At finite- $T$ , an ansatz is used for  $T_{cf}$  and yet the agreement is good to within 94%. Hence we conclude that the CHNC  $n(r)$  is as  $N$ -representable as the DQMC procedure.

The classical pair potential  $U(r) = \mathcal{P}(r) + V_{cou}(r)$  may be used in a classical molecular dynamics simulation to generate the interacting  $g(r)$  instead of using the HNC equations. Such a procedure can reveal crystal ground states and go beyond the liquid-model inherent in the usual HNC equations. It is also possible to generate the dynamics of fluid states, e.g., determine  $S(k, \omega)$  by a classical simulation. However, the Pauli exclusion interaction is really a kinematic quantum effect and not a true ‘interaction’. It is not known at present whether such a classical map  $S(k, \omega)$  agrees in detail with the quantum  $S(k, \omega)$  for an interacting electron fluid.

### CHNC METHOD FOR SYSTEMS OF INTERACTING ELECTRONS AND IONS

In this section the UEL model is extended to two interacting subsystems, namely electrons and ions, or possibly for electrons and holes. The application of the CHNC method to coupled electron-ion system will be illustrated by calculations of hydrogen plasmas where the CHNC results are compared with NPA calculations, as well as recent QMC, PIMC, DFT-MD and other  $N$ -center simulation methods. The CHNC, NPA and Quantum-simulation methods are in good agreement. This agreement is the basis of our second argument for the  $N$ -representability of the pair-densities obtained from the CHNC method.

Consider the two coupled density functional equations of the NPA, viz., Eqs. 5. As shown in the appendix to Ref. [4] these equations for  $n(r), \rho(r)$ , when applied to classical particles reduce to classical Kohn-Sham equations which are Boltzmann like distributions. In the classical case they can be reduced to two coupled HNC-like equations for the electrons and ions. The HNC equation (with or without a Bridge term) for the electrons when replaced by their classical map gives the CHNC equation which now includes an electron-ion contribution to the potential of mean force. Similarly, the HNC-like equation for the ions will contain contributions from the electrons. That is, the electron screening of the ions, or ion screening of the electrons is controlled by the CHNC equations, which only needs the basic pair interactions. If the particles are in the quantum regime, a Pauli-exclusion potential is needed, be it for electrons, or for protons (or holes in semiconductor applications).

As an example, we take a system of ions of mean charge  $\bar{Z}$ , mass  $M$ , with a mean density  $\bar{\rho}$  interacting with a system of electrons at a mean density  $\bar{n} = \bar{Z}\bar{\rho}$ . The

electron mass is unity (atomic units). For simplicity we assume that there is just one kind of ion, and that  $\bar{Z} = 1$  as for a hydrogenic system. We denote the ion species by  $p = H^+$ . The coupled CHNC equations are given in Eq. 34 and in Refs. [41, 42]. They are discussed below.

The densities  $\bar{\rho}$  and  $\bar{n}$  are equal since the ion charge  $\bar{Z} = 1$ . Consider a fluid of total density  $n_{tot}$ , with three species, electrons of two types of spin,  $n_s = \bar{n}/2$  for  $s = 1, 2$  for the two spin species, and  $s = 3, n_3 = \bar{\rho}$  for the ions, denoted here as ‘p’. The physical temperature is  $T$ , while the classical-fluid temperature of the electrons,  $T_{cf} = T_{ee} = 1/\beta_{ee}$ , with  $1/\beta_{ee} = \sqrt{(T^2 + T_q^2)}$ . For the ion  $p = H^+$ , no quantum correction is usually needed and  $T_{pp} = 1/\beta_{pp}$  is  $T$ . Otherwise an ion-quantum temperature  $T_{qp}$  is defined as before, using Eq. 20, but using the Fermi Energy  $E_{Fp}$  of the ions (or holes). If the densities are those typical of stellar densities, then the calculation will automatically be for quantum hydrogen ions as appropriate. Normally, treating the positively charged counter particles of the electrons quantum mechanically is not needed except in semi-conductor structures.

Thus the classical map converts the system with the physical temperature  $T$  into a system with two temperatures  $T_{ee}, T_{pp}$  associated with the two different subsystems. It should be noted that the temperature is not an observable in pure quantum systems as there is no operator associated with it. But it a Lagrange multiplier in quantum *statistical* systems and ensures the conservation of the energy of each subsystem when coupled to classical heat baths where it is measurable. Thus two Lagrange multipliers are implied in the electron-ion system. However, the cross subsystem temperature  $T_{ep}$  is not easily defined as there is no uniform density or specific energy associated with the cross-interactions, and no conserved quantity to define a Lagrange multiplier. It can however be unambiguously extracted from an NPA calculation or constructed from a suitable physical model, as discussed below. So, using  $T_{ij} = 1/\beta_{ij}$  and  $\phi_{ij}$  for the interparticle temperatures and pair-potentials, the coupled CHNC and OZ equations for the PDFs are:

$$g_{ij}(r) = e^{[-\beta_{ij}\phi_{ij}(r) + h_{ij}(r) - c_{ij}(r) + B_{ij}(r)]} \quad (34)$$

$$h_{ij}(r) = c_{ij}(r) + \sum_s n_s \int d\mathbf{r}' h_{i,s}(|\mathbf{r} - \mathbf{r}'|) c_{s,j}(\mathbf{r}') \quad (35)$$

The pair potential  $\phi_{ij}(r)$  between electrons is just the diffraction corrected Coulomb potential  $V_{cou}(r)$  added to the Pauli exclusion potential which vanishes as the de Broglie radius of the particles becomes negligible in approaching the classical regime. The interaction between two ions is also a Coulomb potential with a diffraction correction with a very small length scale ( $\sim 1/\sqrt{M}$ ) due to the mass  $M$  of the ions.

The HNC is sufficient for the uniform 3-D electron liquid for a range of  $r_s$ , up to  $r_s = 50$ , as shown previously [56]. But the bridge term is important for the ions at high compressions and low temperatures. Hence we

neglect the  $e$ - $e$  bridge corrections in this study, but retain them for ions.

The construction of  $\beta_{ep}, \phi_{ep}(r)$  requires attention. Only the product,  $\beta_{ep}\phi_{ij}(r)$  is unambiguously available from the theory, and that is necessary and sufficient for CHNC calculations. However, simple electron-ion interaction models may also be used. Thus Bredow *et al.* [42] examined the applicability of a very simple electron-ion interaction and a simple model for the inter-subsystem temperature of the two-temperature classical map.

$$\phi_{ep}^0(r) = U(r)\{1 - \exp(-r/\lambda_{ep})\}, \quad (36)$$

$$U(r) = (-\bar{Z}/r)f(r), \quad f(r) = 1. \quad (37)$$

$$\lambda_{ep} = (2\pi\bar{m}T_{ep})^{-1/2}, \quad \bar{m} = 1., \quad (38)$$

$$T_{ep} = (T_{ee}T_{pp})^{1/2}. \quad (39)$$

The e-p de Broglie length  $\lambda_{ep}$  moderates the  $r \rightarrow 0$  behaviour of the electron-proton interaction. The latter includes a pseudopotential  $U(r)$  where the form factor  $f(r)$  is set to one for the linear-response regime. For ions with a bound core of radius  $r_c$ , the form factor can be chosen to have the Heine-Abarankov form. In such cases the diffraction correction becomes irrelevant.

Equation 39 for  $T_{ep}$  as a geometric mean of the inter-subsystem temperatures is justifiable in the large- $r$  or small- $k$  limit using compressibility sumrule arguments [66, 67]. However, for small- $r$ , binary collisions dominate and the ansatz becomes less valid. Furthermore the electron density near the nucleus is large, and the effective  $T_{ee}$  increase from the bulk value. Hence a single  $T_{ep}$  is not strictly possible but found to work quite well, as shown below. The ion-ion PDF is insensitive to the choice of  $T_{ep}$ , and hence the model, Eq. (35), proves to be very convenient.

We display the results from the simple model, Eq. 36 in Fig. 3 and compare them with the results from NPA calculations as well as with highly computer-intensive QMC simulations by Liberatore *et al.* [69]. Liberatore *et al.* assume a linear-response form for the proton-electron interaction following the Hammerberg-Ashcroft model of 1974 [70]. Such a model is normally questionable for protons in an electron gas, as the proton-electron interaction is highly nonlinear [71, 72]. A calculation inclusive of all non-linear effects is available from the NPA model, and displayed in Fig. 4(a) for a single proton, confirming that linear-response is accurate at this density. Figure 3 shows that the NPA and CHNC agree accurately with each other and with quantum simulations. While the non-linear CHNC procedure gives good agreement with the QMC results of  $g_{pp}$ , bridge corrections are needed for the form of the ion-ion pair potential used in the NPA, when excellent agreement is obtained, both for the positions of the peaks and the peak heights. The Gibbs-Bogoliubov-LFA criterion determines  $\eta = 0.475$  for this  $\sim 350$ -times compressed hydrogen fluid. The  $g_{ee}$  and  $g_{ep}$  are insensitive to bridge corrections. However, as expected, the

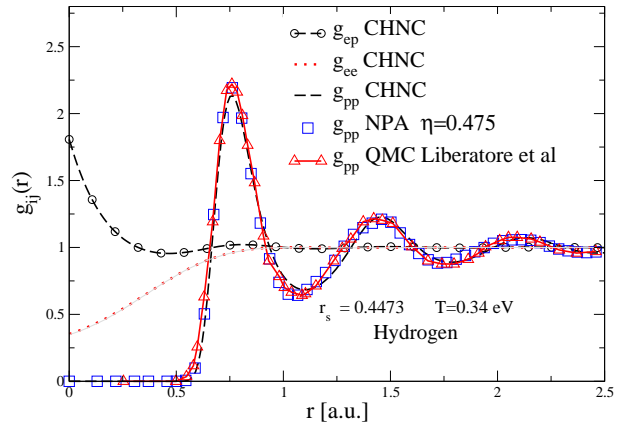


FIG. 3. Pair distribution functions  $g_{ij}(r)$ ,  $i = e, p$  using the simple CHNC model  $T_{ep}, \phi_{ep}$  from Eq. 36, from the NPA, and from QMC (Liberatore *et al.* [69]), for fully ionized hydrogen. The ion density is  $\bar{\rho} = 1.8 \times 10^{25} \text{ cm}^{-3}$  (i.e.,  $\sim 350$  times the density of solid hydrogen) with  $T = 0.34 \text{ eV}$ . The NPA, CHNC and QMC agree very well for  $g_{pp}$  when Bridge corrections specified by the hard-sphere packing fraction  $\eta$  are included in the NPA. See Fig. 4 for more details on  $g_{ep}$

accuracy of  $g_{ep}$  depends on the choice of  $\beta_{ep}\phi_{ep}(r)$ . In Fig. 4(b) we see that the ansatz given by Eq.(35) works well even half-way into the Wigner-Seitz (WS) sphere of the electron with the WS radius  $r_s = 0.4473$ . Hence the classical map is quite accurate for equation of state, transport and other calculations of compressed hydrogen in a highly quantum regime.

The assumptions in Eq. 36. that  $T_{ep} = \sqrt{T_{ee}T_{ii}}$ ,  $\phi_{ep} = Z\{1 - \exp(-r/\lambda)\}/r$ , can be avoided if NPA inputs can be used. For instance, in Ref. [41] the free-electron NPA density  $n(r \rightarrow 0)$  was used to fix  $\lambda_{ep}$ . A more complete approach is also possible. Thus, if the free-electron density increment around one  $H^+$  ion as calculated from the NPA is  $\Delta n_{npa}(r)$ , then we define the  $g_{ep}[\text{one } H^+](q)$  as follows and invert it by the HNC equation to obtain the effective e-p potential  $\beta_{ep}\phi_{ep}$ .

$$h_{ep}[\text{one } H^+](q) = \Delta n_{npa}(q, T)/\bar{n} \quad (40)$$

$$g_{ep}(r) = 1 + h_{ep}(r) = 1 + \Delta n_{npa}(r)/\bar{n} \quad (41)$$

$$\beta_{ei}\phi_{ep}(r) = \text{hnc inversion of: } g_{ep}(r) \quad (42)$$

In Eq. 42 we imply that the  $g_{ep}(r)$  is now interpreted as a classical PDF in a system containing protons and electrons. It is HNC-inverted to obtain the classical pair-potential  $\beta_{ep}\phi_{ep}(r)$  in a manner analogous to the extraction of the Pauli potential from  $g_{ee}^0(r)$ . However, in the regime of high compressions, the model of Eq. 36 seems to be sufficient.

While the NPA and CHNC calculations agreed with the QMC results of Liberatore *et al.* in the linear-response regime, we show that similar agreement is found in regimes where linear response does not hold. In Fig. 5 we show that the PDFs obtained using our single-center

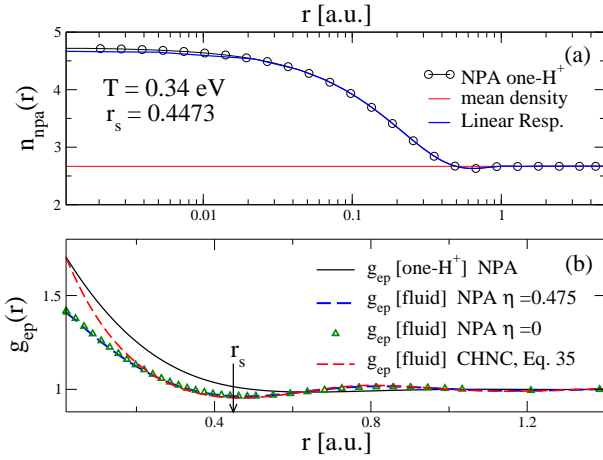


FIG. 4. (a) The free-electron density  $n_{\text{npa}}(r)$  calculated from the NPA model at a proton in a hydrogen plasma,  $T = 0.34$  eV, with an ion density of  $\bar{\rho} = 1.8 \times 10^{25}$  cm<sup>-3</sup>, i.e.,  $r_s = 0.4473$ . At this high density linear-response theory (dashed curve) is accurate. (b) The density displacement can be used to define  $g_{\text{ep}}(r)$  for the one-proton system and its generalization to the fluid. Results for  $g_{\text{ep}}$  obtained from a simple model of Eq. 36 within the CHNC, and calculations from the NPA for hydrogen fluid using the MHNC equation are displayed.

approaches agree very well with highly computer intensive quantum simulations, e.g., those of Morales *et al.* [73] using coupled electron-ion Monte Carlo calculations with 54 protons in the simulation cell. The  $g_{\text{pp}}(r)$  of such quantum simulations are limited by the simulation cell size, while the NPA calculations capture the effect of many Friedel oscillations in the potentials. Our results imply that the ion-ion correlation functionals used in the single-center NPA method to incorporate many-ion effects are successful. This has also been verified in many other calculations during past decades, even with respect to complex fluids like warm dense carbon, silicon etc., where there are covalent bonding effects as well [27, 28]. A similar verification is available in the context of ion-dynamical calculations [74, 75]. The NPA and CHNC methods are not limited by the Born-Oppenheimer approximation, as the static effects of the electron-nuclear coupling can be incorporated in the electron-ion correlation functionals [76].

The quantum simulation method used by Morales *et al.* is described by them as “a QMC based ab initio method devised to use QMC electronic energy in a Monte Carlo simulation of the ionic degrees of freedom.... Specifically, the use of twist averaged boundary conditions (TABCs) on the phase of the electronic wave function, together with recently developed finite-size correction schemes, allows us to produce energies that are well converged to the thermodynamic limit with 100 atoms”. More detailed calculations using CHNC, NPA, and comparisons of the resulting thermodynamic data (calculated from the

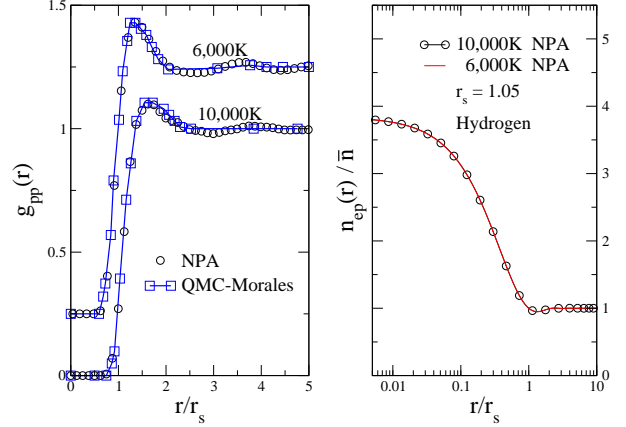


FIG. 5. (b) The fractional free-electron density  $n_{\text{npa}}(r)/\bar{n}$  or  $g_{\text{ep}}$  at a single proton calculated from the NPA model at a proton in a hydrogen plasma at  $r_s = 1.05$  a.u. This is effectively unchanged between  $T = 6,000$  and  $10,000$  K (b) The NPA density displacement can be used to define a pseudopotential for the one-proton system and the fluid  $g_{\text{pp}}$  is calculated using an ion-correlation functional which reduces to the HNC diagrams, as the Bridge corrections are negligible in this case. Results agree closely with the coupled electron-ion quantum Monte Carlo simulations of Morales *et al.* [73] which are however limited by the size of the simulation box. Only the case  $r_s = 1.05$  is shown.

PDFs using coupling constant integrations) will be taken up elsewhere.

## SYSTEMS WHERE ALL PARTICLES ARE IN THE QUANTUM REGIME

If both subsystems, viz., ions and electrons are in the quantum regime, this poses no additional difficulty for the CHNC method. However, in practice, such quantum corrections for ions in the liquid state are possible only under extreme compressions, even for hydrogen, and such compressions are only available in astrophysical settings.

On the other hand, in electron-hole systems as found in semiconductor materials, the quantum nature of both types of particles must be included as the hole masses (empty states in the valence band) are usually within a factor of ten of the electron mass. Furthermore, if the electrons and holes are confined in two quantum wells separated by a thin insulating barrier, the spontaneous recombination of electrons and holes is suppressed. Such systems can be fabricated and are known as double quantum wells (DQWs) where the electrons occupy the lowest conduction subband in one of the wells, while the holes occupy the highest valence subband in the other well. They form two interacting but spatially

TABLE I. Characteristic quantities for electrons and holes in a typical GaAs/GaAlAs in a double quantum well structure. These are examples for 2-dimensional warm dense matter states where the electron and its positive counter particle behave quantum mechanically. The material dielectric constant  $\varepsilon=12.9$  for both layers separated by an AlAs barrier of 10 nm width and held at a temperature  $T = 5K$ . Each layer has its effective Bohr radius and effective Hartree unit. So  $r_s, E_F$  etc., are expressed in the respective effective units. The classical strong coupling parameter  $\Gamma = 1/(r_s T_{cf})$  is given.

item	electron layer	hole layer
Particle density ( $\text{cm}^{-2}$ )	$4 \times 10^{11}$	$4 \times 10^{11}$
Effective mas $m_s^* = m_s/m_0$	0.0670	0.3350
Layer width (nm)	15.00	20.00
Effective $r_s$	2.768	13.84
Effective $E_F$	0.1304	$0.5218 \times 10^{-2}$
degeneracy parameter $T/E_F$	0.3015	1.508
Classical fluid temp. $T_{cf}/E_F$	1.966	2.188
Inverse de Broglie Length	1.180	0.1807
Plasma coupling parameter $\Gamma$	1.408	6.327

separated 2-D electron fluids. Properties of such DQWs in the symmetric case, (i.e., for the case where the electron and hole masses  $m_e, m_h$ , well widths  $w_e, w_h$ , layer dielectric constants and temperatures are equal) have already been studied using the CHNC method [43]. However, in typical GaAs-GaAl $_x$ As $_{1-x}$  DQWs, the electron and hole masses are, typically, 0.067 and 0.335, respectively, while the material dielectric constant  $\varepsilon$  is taken as  $\sim 12.9$  for the whole structure since the aluminum alloy content  $x$  is small. The barrier dielectric constant is typically about 12.62. The effective Bohr radius is given by  $a_B^* = \hbar^2 \varepsilon / (m_0 e^2 m_s^*)$  where  $m_0$  is the free-electron mass while  $m_s^*$  is the effective mass of the species ‘s’. Typical well widths  $w$  and barrier widths are 10-30 nm. Given these material properties, a DQW with equal densities of electrons and holes at a temperature of even 5K is found to be a two component interacting partially degenerate system where the  $r_s, E_F$  values, and hence the degeneracies are widely different (see Table 1). In fact, these DQWs provide excellent laboratory examples of 2-dimensional interacting warm dense matter. They contain four interacting subsystems as the electrons, and holes are spin 1/2 fermions for GaAs/GaAlAs DQWs, but there is no exchange interaction between particles in separate layers. Such DQWs can be made with two electron layers, two hole layers, or an electron layer coupled to a hole layer. For more computational details, see Ref. [43].

These systems are of great interest in nanostructure physics as the transport properties, plasmon dispersion, energy relaxation etc., depend on the corresponding structure factors and local-field corrections which enter into response functions and effective potentials. All

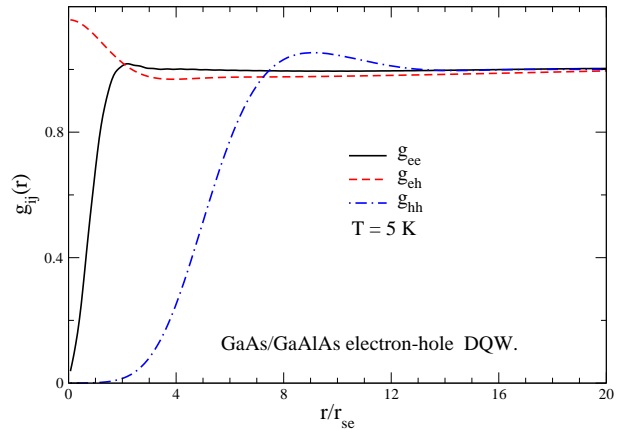


FIG. 6. The  $e$ - $e$ ,  $e$ - $h$  and  $h$ - $h$  pair distribution functions  $g(r)$  for an electron layer interacting with a hole layer in a GaAs/GaAlAs double quantum well maintained at 5K. The  $x$ -axis is in units of the electron Wigner-Seitz radius  $r_{se} = 2.768$  in units of the effective electron atomic unit of length (materials details are given in Table 1). This is an example of quasi two-dimensional warm dense matter, realized at 5K.

such quantities can be extracted from CHNC calculations [5, 43]. Currently, the CHNC technique is the only method available for treating such systems at arbitrary layer degeneracies, spin polarizations, and arbitrary effective masses at zero to finite temperatures. The pair-distribution functions for the spin unpolarized  $e$ - $h$  DQW system described in Table 1 are displayed in Fig. 6. Unfortunately, QMC or other microscopic calculations for such systems are believed to be too prohibitive at present, and no comparisons are available.

#### The $N$ -representability and $v$ -representability of CHNC densities for electron-ion systems

The  $N$ -representability of the electron-electron  $g_{ee}(r)$  obtained from the CHNC method for electron-ion systems needs to be examined. This too can be approached as in the previous section. It appears that  $N$ -representability is preserved in this case too, where we have merely made the electrons to interact with the ‘external potential’ of the ions which is, however, self-consistently adjusted in the two component problem, with no invoking of the Born-Oppenheimer approximation. The BO corrections come through the electron-ion correlation potentials (HNC-like diagrams) contained in the HNC equation describing the  $g_{ep}(r)$  pair distribution function [76].

We may also note that the  $v$ -representability of the densities generated by CHNC, or via the NPA can be treated using standard methods since we are dealing entirely with Coulombic systems and spherical charge densities. For such systems, Kato’s theorem [77] applies, and the methods based on spherical densities due to

Theophilou, Nagy *et al.* can be used [78, 79].

## CONCLUSION

A review of the classical map hypernetted chain procedure, which is a way of side stepping the construction of a quantum kinetic energy functional for density functional theory, or doing quantum calculations is presented. A proof of the  $N$ -representability of the classical map, and plausibility arguments for  $N$ -representability are given based on agreement of CHNC results with QMC and other bench mark results. The application of the CHNC method to general electron-ion systems is reviewed. Computationally demanding quantum systems like warm dense matter become numerically very simple and rapid within the CHNC method. The classical map may be used without the HNC procedure, via classical MD simulations. Thus, within certain limits, entirely classical calculations which are very rapid and independent of the number of particles and the system temperature are possible for a wide class of quantum problems.

The author thanks Professors Sam Trickey and Jim Dufty for raising the question of the  $N$ -representability of the CHNC procedure at the CECAM workshop at Lausanne, Switzerland, in May 2019.

---

\* Email address: chandre.dharma-wardana@nrc-nrc.gc.ca

- [1] Ziman, J. M. *Adv. Phys.* **13**, 89 (1964)
- [2] L. Dagens, *J. Phys. (Paris)* **36**, 521 (1975).
- [3] J. Chihara, *J. Phys. C* **18**, 3103 (1985)
- [4] M. W. C. Dharma-wardana and F. Perrot, *Phys. Rev. A* **26**, 2096 (1982).
- [5] M. W. C. Dharma-wardana and F. Perrot, *Phys. Rev. Lett.* **84**, 959 (2000)
- [6] A. J. Coleman, *Rev. Mod. Phys.* **35**, 668 (1963).
- [7] R. Erdahl and V. H. Smith Jr., Eds., *Density Matrices and Density Functionals: Proceedings of the A. John Coleman Symposium* (Reidel, Boston, 1987).
- [8] F. Perrot and M. W. C. Dharma-wardana, *Phys. Rev. A* **30**, 2619 (1984).
- [9] P. Hohenberg and W. Kohn. *Phys. Rev.*, **136**, B864 (1964).
- [10] W. Kohn and L. J. Sham, *Phys. Rev.* **140**, A1133 (1965).
- [11] R. M. Dreizler and E. K. U. Gross, *Density Functional Theory*, (Springer, Berlin, 1990).
- [12] P. Vashista and W. Kohn, Eq. C.7, Ch. 2 in *Theory of the Inhomogeneous electron gas*, Eds. S. Lundqvist and N. H. March, Plenum, New York (1983)
- [13] N. D. Mermin, *Phys. Rev. B* **1**, 2362 (1970).
- [14] K. Capelle and G. Vignale, *Phys. Rev. Lett.* **86** 5546 (2001).
- [15] Louis Garrigue, arXiv:1906.03191v1 [math-ph] (2019).
- [16] Joseph E. Mayer, *Phys. Rev.* **97** 1579 (1955).
- [17] M. Levy. *Phys. Rev. A*, **26**, 1200, (1982).
- [18] D. A. Mazziotti, *Phys. Rev. Lett.* **108**, 263002 (2012).
- [19] B. B. L. Witte, P. Sperlring, M. French, V. Recoules, S. H. Glenzer, and R. Redmer, *Physics of Plasmas* **25**, 056901 (2018).
- [20] Y. A. Wang and E. A. Carter, Chapter 5 of *Theoretical Methods in Condensed Phase Chemistry*, in book series of *Progress in Theoretical Chemistry and Physics*, edited by S. D. Schwartz, pp. 117-184 (Kluwer, Dordrecht, 2000).
- [21] V. V. Karasiev, T. Sjostrom, and S. B. Trickey, *Phys. Rev. B* **86**, 115101 (2012).
- [22] T. G. White, S. Richardson, B. J. B. Crowley, L. K. Pattison, J. W. O. Harris, and G. Gregori, *Phys. Rev. Lett.* **111**, 175002 (2013).
- [23] Jouko Lehtomäki, Ilja Makkonen, Miguel A. Caro, Ari Harju, and Olga Lopez-Acevedo, *J. Chem. Phys.* **141**, 234102 (2014). [<http://dx.doi.org/10.1063/1.4903450>].
- [24] J. Cl rouin Gr gory Robert, Philippe Arnault, Christopher Tricknor, Joel D. Kress, and Lee A. Colins *Phys. Rev. E* **91** 011101(R), (2015).
- [25] E. K. U. Gross, and R. M. Dreizler, *Density Functional Theory*, NATO ASI series, **337**, p 625, Plenum Press, New York (1993).
- [26] F. Perrot and M.W.C. Dharma-wardana, *Phys. Rev. E.* **52**, 5352 (1995).
- [27] M. W. C. Dharma-wardana and F. Perrot, *Phys. Rev. Lett.*, **65**, 76 (1990).
- [28] M. W. C. Dharma-wardana, *Contrib. Plasma Phys.* **58** 128-142 (2018).
- [29] M. Ishitobi and J. Chihara, *J. of Physics: Condensed matter*, **4** 3679 (1992).
- [30] J. A. Anta and A. A. Louis, *Phys. Rev. B* **61**, 11400 (2000).
- [31] Hong Xu and J. P. Hansen, *Physics of Plasmas* **9**, 21 (2002).
- [32] J. Chihara, *Progress in Theoretical Physics* **72**, 940 (1984).
- [33] G. Kresse and J. Furthm ller, *Phys. Rev. B* **54**, 11169 (1996).
- [34] X.Gonze and C. Lee, *Computer Phys. Commun.* **180**, 2582-2615 (2009).
- [35] M. Levy and HuiOu-Yang, *Phys. Rev. A* **38**, 625 (1988).
- [36] V. Karasiev, S. Trickey, and F. Harris, *J. Comput. Aided Mater. Des.* **13**, 111 (2006).
- [37] C. J. Umrigar and Xavier Gonze, *Phys. Rev. A* **50**. 3827 (1994).
- [38] Fran ois Perrot and M. W. C. Dharma-wardana, *Phys. Rev. Lett.* **87**, 206404 (2001).
- [39] C. Bulutay and B. Tanatar, *Phys. Rev. B* **65**, 195116 (2002).
- [40] Chieko Totsuji, Takashi Miyake, Kenta Nakanishi, Kenji Tsuruta and Hiroo Totsuji, *J. Phys.: Condens. Matter* **21** 045502 (2009).
- [41] Dharma-wardana, M. W. C. and Perrot, F. *Phys. Rev. B* **66**, 014110 (2002).
- [42] R. Bredow, Th. Bornath, W.-D. Kraeft, M.W.C. Dharma-wardana and R. Redmer *Contributions to Plasma Physics*, **55**, 222-229 (2015).
- [43] M. W. C. Dharma-wardana, D. Neilson and F. M. Peeters, *Phys. Rev. B* **99**, 035303 (2019). <https://arxiv.org/abs/1901.00895>
- [44] G. D. Mahan, *Many particle Physics*, Sec. 5.1, Plenum Publishers, New York (1981).
- [45] G. F. Giuliani and G. Vignale, *Quantum Theory of the Electron Liquid.*, Appendix 4, Cambridge University Press (2005).
- [46] M. W. C. Dharma-wardana and F. Perrot, *Phys. Rev. B*

- 70**, 035308 (2004).
- [47] M. W. C. Dharma-wardana and François Perrot, *Europhys. Letters*, **63**, 660 (2003).
- [48] M. W. C. Dharma-wardana, *Phys. Rev. B* **72**, 125339 (2005).
- [49] F. Lado, *J. Chem. Phys.* **47**, 5369 (1967).
- [50] M. W. C. Dharma-wardana, *J. Phys. Conf. Ser.* **442**, 012030 (2013).
- [51] Dharma-wardana, M. W. C. and Aers, G. C., *Phys. Rev. Lett.* **56**, 1211 (1986).
- [52] Yaakov Rosenfeld and Gerhard Kahl, *J. Phys.: Condens. Matter* **9** L89, (1997).
- [53] H. Minoo, M. M. Gombert, and C. Deutsch, *Phys. Rev. A* **23**, 924 (1981).
- [54] Singwi, M. P. Tosi, R. H. Land, and A. Sjölander, *Phys. Rev.* **176**, 589 (1968).
- [55] P. Vashista and K. S. Singwi, *Phys. Rev. B* **6**, 875 (1972).
- [56] F. Perrot and M. W. C. Dharma-wardana, *Phys. Rev. B* **62**, 16536 (2000); *Erratum:* **67**, 79901 (2003); arXiv-1602.04734.
- [57] F. Lado, S. M. Foiles and N. W. Ashcroft, *Phys. Rev. A* **28**, 2374 (1983).
- [58] Yu Liu and Jianzhong Wu, *J. Chem. Phys.* **141**, 064115 (2014).
- [59] J. Dufty, and S. Dutta, *Phys. Rev. E* **87**, 032101 (2013).
- [60] G. Kelbg, *Ann. Phys.* **467**, 219 (1963).
- [61] A. V. Filinov, V. O. Golubnychiy, M. Bonitz, W. Ebeling, and J. W. Dufty, *Phys. Rev. E* **70**, 046411 (2004).
- [62] Tobias Dornheim, Simon Groth, Michael Bonitz *Physics Reports*, **744**, 1-86 (2018), <https://doi.org/10.1016/j.physrep.2018.04.001>.
- [63] E. W. Brown, J. L. DuBois, M. Holzmann and D. M. Ceperley, *Phys. Rev. B* **88**, 081102(R) (2013).
- [64] V. V. Karasiev, T. Sjöstrom, J. W. Dufty, and S. B. Trickey, *Phys. Rev. Lett.* **112**, 076403 (2014).
- [65] S. Groth, T. Dornheim, T. Sjöstrom, F.D. Malone, W. M. C. Foulkes, M. Bonitz, *Phys. Rev. Lett.* **119** (13) 135001 (2017). <http://dx.doi.org/10.1103/PhysRevLett.119.135001>.
- [66] Nathaniel R. Shaffer, Sanat Kumar Tiwari, and Scott D. Baalrud, *Phys. of Plasmas* **24**, 092703 (2017).
- [67] R. Bredow, T. Bornath, W.-D. Kraeft, and R. Redmer, *Contrib. Plasma Phys.* **53**, 276 (2013).
- [68] E. H. Lieb, *Int. J. Quant. Chem.* **24**, 243 (1983).
- [69] E. Liberatore, C. Pierleoni, and D. Ceperley, *J. Chem. Phys.* **134**, 184505 (2011).
- [70] J. Hammerberg and N. W. Ashcroft, *Phys. Rev. B* **9**, 409 (1974).
- [71] P. Jena and K. S. Singwi *Phys. Rev. B*, **17** 1592 (1978).
- [72] F. Perrot *Phys. Rev. A* **25**, 489 (1982).
- [73] Miguel A. Morales, Carlo Pierleoni, and D. M. Ceperley *Phys. Rev. E* **81** 021202 (2010).
- [74] F. Nardin, G. Jacucci and M.W.C. Dharma-wardana, *Phys. Rev. A* **37**, 1025-1028 (1988) [NRCC 28307].
- [75] L. Harbour, and G. D. Förster, M. W. C. Dharma-wardana, and L. J. Lewis, *Physical review E* **97**,043210 (2018). DOI: 10.1103/PhysRevE.97.043210 (2018).
- [76] F. Perrot, Y. Furutani and M.W.C. Dharma-wardana, *Phys. Rev. A* **41**, 1096-1104 (1990).
- [77] T. Kato, *Commun. Pure Appl. Math.* **10**, 151 (1957).
- [78] A. Theophilou, *J. Chem. Phys.* **149**, 074104 (2018).
- [79] A. Nagy, *J. Chem. Phys.* **149**, 204112 (2018).